CHEMICAL ENGINEERING TRANSACTIONS
VOL. 94, 2022
A publication of AIDIC
The Italian Association of Chemical Engineering
Online at www.cetjournal.it
Guest Editors: Petar S. Varbanov, Yee Van Fan, Jiří J. Klemeš, Sandro Nižetić

ISBN 978-88-95608-93-8; **ISSN** 2283-9216
DOI: 10.3303/CET2294228

Effect of Flow Pattern in Superstructure-Based Optimisation of Fixed-Site Carrier Membrane Gas Separation During Post-Combustion CO_2 Capture

Natsayi Chiwaye[a]*, Thokozani Majozi[a], Michael O. Daramola[b]

[a]NRF/DST Chair: Sustainable Process Engineering, School of Chemical and Metallurgical Engineering, Faculty of Engineering and the Built Environment, University of the Witwatersrand, Wits 2050, Johannesburg, South Africa
[b]Department of Chemical Engineering, Faculty of Environment, Built Environment and Information Technology, University of Pretoria, Hatfield 0028, Pretoria, South Africa
natsayichiwaye@gmail.com

Membrane-based gas separation continues to be an area of interest that is being explored for various applications and efforts are being made to enable large-scale implementation and commercialisation. Works on techno-economic studies in areas such as carbon capture, natural gas sweetening, and biogas upgrading has been reported. Various simulation studies have reported the effect of the membrane flow pattern on permeate recovery and purity. The simulation studies in this area have been limited to single-stage and two-stage membrane processes, while many of these studies considered polymer membranes, facilitated transport has barely been investigated. In addition, optimisation studies that compared different flow patterns in the membrane module have been few. The facilitation of gas permeation decreases as pressure is increased due to carrier saturation. However, an increased pressure increases the driving force, and a trade-off should be achieved. The different membrane flow patterns also have inherent driving force potential. In this work, a superstructure-based model that also embeds a fixed site carrier permeation membrane has been developed for CO_2 capture from a coal-fired power plant and three scenarios based on the different flow patterns, i.e., co-current, counter-current and crossflow, were analysed to determine the effect of the flow pattern in the membrane module. The main objective of the optimisation was to minimise the cost of capture. The counter-current flow pattern resulted in the lowest cost of capture as it resulted in the most energy-efficient process system. The co-current flow-based optimisation results in configuration result in an 18 % increase in cost compared to the counter-current flow pattern optimisation run due to a 29 % increase in energy consumption. The crossflow pattern optimisation results in a 9 % increase in the annualised cost of capture compared to the counter-current flow.

1. Introduction

Membranes to separate gas mixtures are ever becoming popular as new membranes are being tested for various applications. Polymer membranes have great potential since they can be modified to enhance the permeance and selectivity of the target component (Liao et al., 2016). Membrane technology has been studied in carbon capture processes such as post-combustion capture from flue gas produced in power plants (He and Hägg, 2014) and cement manufacturing (Dai et al., 2019). Whilst laboratory experimental results are promising, large-scale application faces several challenges. These include pressure drop, membrane degradation and failure at exposure to minor elements whose effect is not usually investigated at the laboratory stage (Yuan et al., 2017). Process design and techno-economic studies, and optimisation are essential steps toward commercialisation. The flow pattern inside the membrane module has always been considered an important part of membrane process design. Rautenbach and Dahm, (1987) reported that the effect of the flow pattern is dependent on the type of application. Merkel et al. (2010) studied different membrane module flow patterns for CO_2 separation from flue gas from coal-fired power plants. The report showed that the counter-current flow resulted in a higher stage cut, requiring a smaller membrane area and lower energy consumption due to enhanced driving force. The process flow pattern is selected beforehand in simulation and optimisation studies

Paper Received: 26 April 2022; Revised: 21 June 2022; Accepted: 23 June 2022
Please cite this article as: Chiwaye N., Majozi T., Daramola M.O., 2022, Effect of Flow Pattern in Superstructure-Based Optimisation of Fixed-Site Carrier Membrane Gas Separation During Post-Combustion CO2 Capture, Chemical Engineering Transactions, 94, 1369-1374 DOI:10.3303/CET2294228

(Stoller and Pulido, 2017). Several superstructure-based optimisation studies have been reported and various flow patterns have been assumed in the studies. For instance, the cross-flow pattern was considered by Velasco et al. (2021) and the co-current flow pattern is often considered in simulation studies due to the simplicity of the resulting model (Hasan et al., 2012). The counter-current flow pattern has also been assumed since previous studies showed that it results in a higher stage cut and purer permeate (Lee et al., 2018). While various authors have reported on the sensitivity of gas separations by membranes to the flow pattern, many have been parametric studies based on one-stage or two-stage studies. Uppaluri et al. (2004) carried out a superstructure optimisation of a multi-stage membrane system for the recovery of H_2 from syngas (H_2+CO_2). The results showed that the counter-current pattern in the membrane module gave the lowest cost of the membrane network, however, the difference was small. Many superstructure-based optimisation studies have analysed polymer membranes and embedded the classic 'solution diffusion model' (Lee et al., 2018). Chiwaye et al. (2021) tackled the more complex task of embedding a fixed-site carrier (FSC) membrane permeation model and considered humidified gas in superstructure-based optimisation of membrane networks. This study builds on that previous work to investigate the effect of flow patterns on the membrane module performance. A superstructure-based model that considers a fixed-site carrier membrane for the separation of CO_2 from flue gas produced in a coal-fired power plant is developed. Three scenarios that include flow pattern models of co-current, counter-current and cross-flow configuration are studied. This information is important in the scale-up studies for the post-combustion CO_2 capture process by FSC membrane.

2. Model development

The problem statement can be summarised as фолловс. Given a flue gas of known composition, temperature and pressure, desired recovery and purity targets; determine the minimum annualised cost of capture considering a specific flow pattern in the membrane module. The model developed is based on the superstructure presented in previous work (Chiwaye et al., 2021). For the model development, it is assumed that pressure and concentration polarisation are negligible, the flue gas to be separated is free of dust and minor components and the membrane operates isothermally (Lee et al., 2018). These assumptions may result in lower estimates of power and membrane area and a more detailed model would have to be applied before scale-up.

2.1 Process description

Figure 1 shows the superstructure that embeds numerous process flow routes.

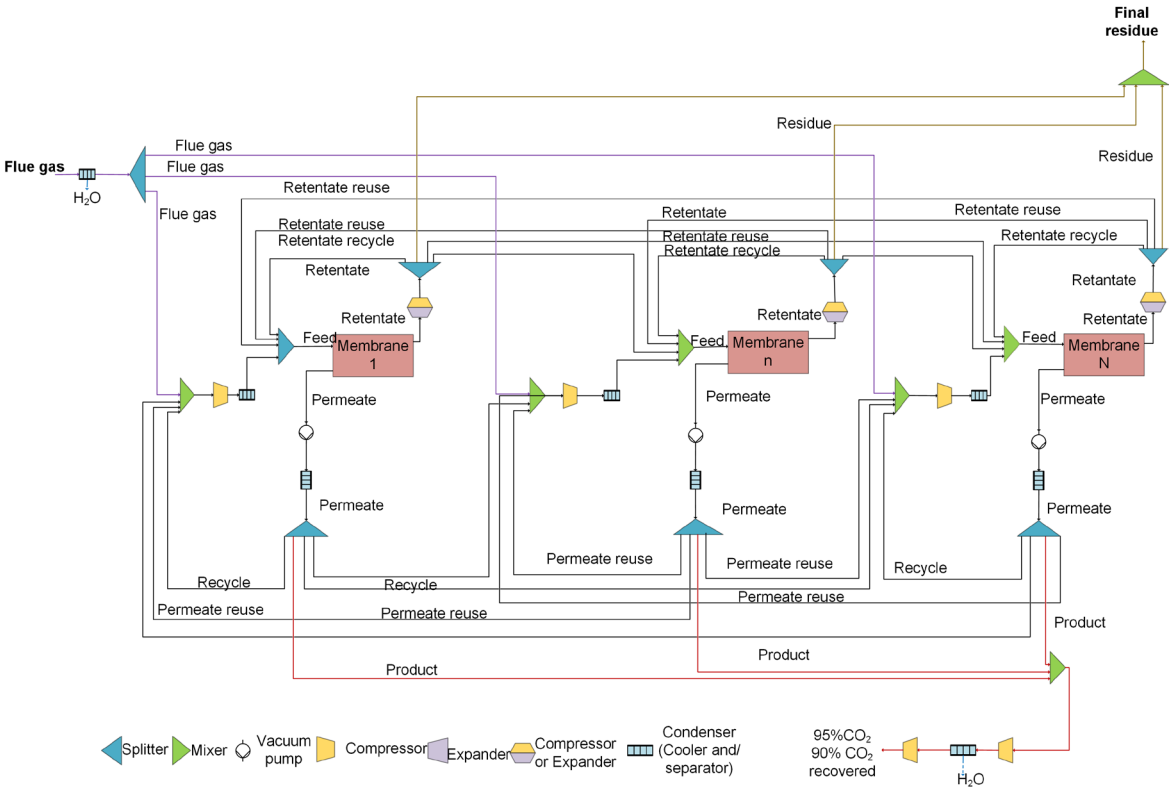

Figure 1: Superstructure, adapted with permission from (Chiwaye et al., 2021)

The flue gas from the power plant (1 bar and 49 °C) is initially cooled down to 25 °C and some water condenses and is removed at that stage. The flue gas can then be split and sent to any of the membranes where it has the potential to mix with the permeate recycle before being compressed to membrane feed pressure. Compressing the gas increases its temperature and is cooled down to the membrane operating temperature (40 °C). Thereafter it is mixed with retentate recycle that has been expanded or compressed to a matching pressure. The mixture makes up the feed and is passed on to the retentate membrane where the gaseous component permeates according to their permeances under the conditions. There is a vacuum pump on the membrane side to enhance the driving force. There are coolers that ensure that the gases are cooled and only mixed at the same temperature. The permeate can be split into the product stream or recycle streams that can be sent to any of the stages. The retentate is also sent to a splitter and can be split into recycle streams or sent to the residue stream as clean effluent to the atmosphere.

2.2 Model development

A superstructure-based optimisation model for the FSC membrane with a counter-current flow pattern in the membrane module was reported by (Chiwaye et al., 2021). Scenarios are developed to include appropriate models for the cross-flow pattern and co-current pattern. The FSC permeation transport model reported by Zhang et al. (2013) is embedded in the model. Polyvinyl-amine supported on polysulfone FSC membrane is considered (Kim et al., 2013). The FSC membrane facilitates CO_2 movement under humid conditions. Therefore, the model includes a constraint that ensures the relative humidity of the feed as supplied to the membrane is greater than 90 % (Kim et al., 2013). The membrane profile is discretised, and the backward finite element method is used to solve for the membrane area (Arias et al., 2016). The complete model based on the counter-current flow pattern in the membrane module that also consists of an FSC CO_2 permeance model is described in previous work (Chiwaye et al., 2021). Based on a similar approach, the material balance around the membrane co-current flow is presented in Eq.(1). The balance shows that the sum of flowrate (R) of the components *(i)* that flow across a point k on the retentate and permeate side is equal to the sum of the components that leave the membrane stage (*n*). The material balance around the membrane operating cross-flow pattern is shown in Eq.(2) and Eq.(3). Eq.(2) shows that the total permeate of a component *(i)* from the membrane is a sum of the permeate from each discretised section.

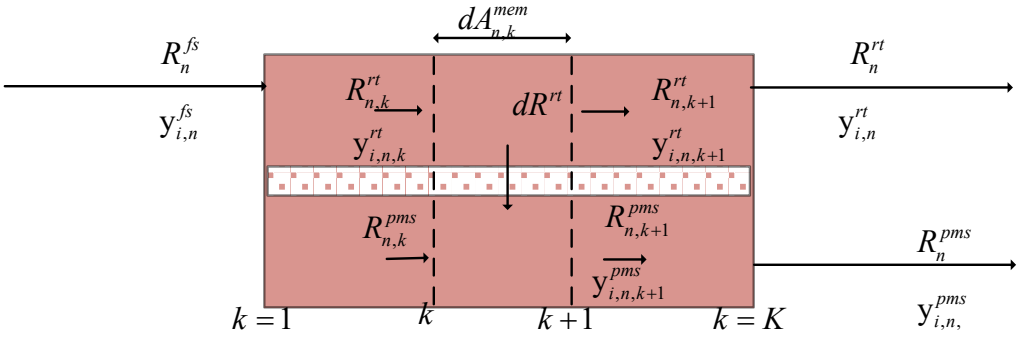

Figure 2: Figure showing flow of components in co-current pattern in the membrane module

$$R^{rt}_{n,k} \cdot y^{rt}_{i,n,k} + R^{pms}_{n,k} \cdot y^{rt}_{i,n,k} = R^{rt}_{n,K} \cdot y^{rt}_{i,n,K} + R^{pms}_{n,K} \cdot y^{pms}_{i,n,K} \quad \forall i \in I; \forall n \in N; k \in K \tag{1}$$

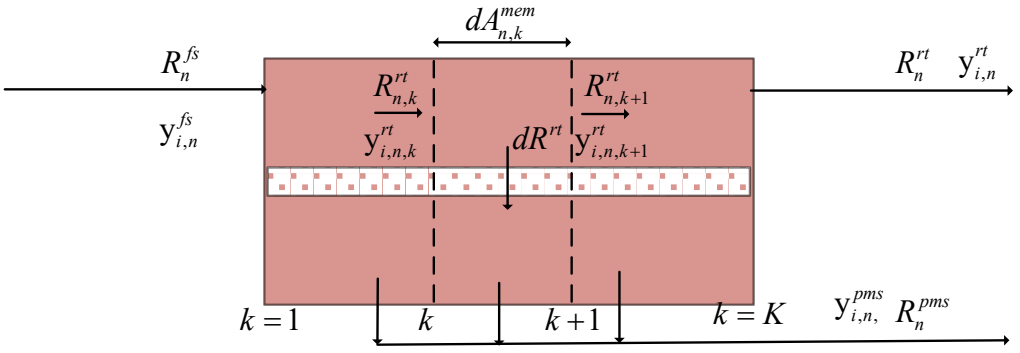

Figure 3: Figure showing the flow of components in the cross-flow pattern in the membrane module

$$R_{i,n}^{pms} = \sum_{k=1}^{K} R_{i,n,k}^{pms} \qquad \forall i \in I; \forall n \in N \tag{2}$$

$$R_{n,k}^{rt} \cdot y_{i,n,k}^{rt} + R_{n,k}^{pms} \cdot y_{i,n,k}^{pms} = R_{n,K}^{rt} \cdot y_{i,n,K}^{rt} + R_{n}^{pms} \cdot y_{i,n}^{pms} \qquad \forall i \in I; \forall n \in N; k \in K \tag{3}$$

Material balances are carried out around the membranes, splitters, and coolers (Uppaluri et al., 2004). The desired recovery and purity are set at 90 % and 95 %. Inequality constraints describing the pressure lower and upper bound for both the retentate and permeate sides are included in the model. Water condenses out of the gases stream when its partial pressure exceeds the saturation pressure as modelled in previous works (Pfister et al., 2017). An equality that limits the water partial pressure to less than the saturation pressure is included to prevent water condensation in the membrane module.

2.3 Objective function

The objective of the optimisation is to minimise the total annual cost (TAC). The TAC is a sum of the CAPEX and the OPEX. The CAPEX is dominated by the membrane area whilst the OPEX mainly reflects the cost of electric power consumed by the compressors. The compressor duties are modelled as commonly reported (Arias et al., 2016).

2.4 Illustrative Example

In order to obtain numerical solutions to the scenarios, CO_2 capture from an existing reference coal-fired plant that produces 819 MW of electricity and flue gas of flowrate 26.61 kmol/s is considered (CESAR, 2011; He and Hägg, 2014). It is assumed that the flue gas is free of NOx and SOx after passing through the deNOx and desulphurisation processes and the effect of minor elements is negligible. In the optimisation runs the flue gas composition was considered as CO_2 12.7 %, N_2 72.9 %, H_2O 9.7 % and O_2 is 3.7 % (He and Hägg, 2014). However, in experimental work, the presence of minor elements results in a decrease in CO_2 permeance (Li et al., 2014). Kim et al., (2013) presented a highly permeable, CO_2 selective FSC membrane and its properties such as membrane thickness are used as input parameters for the CO_2 permeance model as detailed in previous work (Chiwaye et al., 2021). The CO_2 permeance varies with pressure and both are variables that are being optimised. However, the permeances of the other components is constant; (N_2, H_2O and O_2) are 1.84×10^{-7}, 2.48×10^{-5}, 8.26×10^{-7} kmol/ (m^2.bar.s) (Chiwaye et al., 2021). The membrane cost is US$ 35, and the cost of labour is 37 US$/h. The efficiencies of the compressors, vacuum and expanders are assumed to be 85 % whilst the adiabatic compression coefficient considered is 1.4. A capital recovery factor of 0.2 is factored in. The cost of the coolers on the recycle streams and product stream is considered negligible since the process flowrates are lower than the flue gas supplied from the power plant. Membrane and project lifetime are considered to be 5 y and 25 y. The total purchasing cost is inflation-adjusted to 2018 values from the 2012 values. The input data for the reference plant, membrane permeance and cost evaluation are detailed in previous work (Chiwaye et al., 2021). An MINLP model formulated is implemented in the General Algebraic Modelling Systems (GAMS) 37.7 and solved by the solver Branch and Reduce Optimization Navigator (BARON) (Puranik and Sahinidis, 2017).

3. Results and discussions

Three optimisation runs based on three membrane stages for the three flow patterns were carried out. These three scenarios are named after the membrane flow pattern i.e. counter-current as previously reported (Chiwaye et al., 2021), co-current and cross flow. A target recovery of 90 % and product stream purity of 95 % was set, as commonly assumed in other studies (Lee et al., 2018). Table 1 presents the resulting optimum membrane area and pressure for the various membrane stages. The pressure ratios shown indicate that the co-current flow pattern results in the highest retentate operating pressure of the three scenarios. The optimum retentate of one of the membrane stages is highest at 7.65 bar and as such the water mole fraction that satisfies the required relative humidity is lowest for this scenario. The optimum membrane areas are also lower for the optimisation run based on the co-current flow pattern as all the membrane areas are below 0.6 m^2. It follows then that the total membrane area of the co-current flow pattern is lowest at 1.62 $x10^6$ m^2, which is about 16 % lower than both the counter-current and the cross-flow pattern. In a previous parametric study similar observation was made (Khalilpour et al., 2012). As the concentration of the highly permeable component decreases along the retentate side, the other components increase in permeance and dilute the purity of the target component, and a smaller membrane area is preferred to achieve the desired purity.

Table 1: Optimum pressure and membrane area for the different membrane stages for the three scenarios

	Counter-current			Co-current			Cross-flow		
Membrane stages	1	2	3	1	2	3	1	2	3
Membrane area ($x10^6$ m^2)	0.38	0.98	0.38	0.55	0.57	0.35	0.40	1.0	0.37
Retentate (bar)	2.58	4.28	2.58	7.65	3.36	3.36	2.92	4.97	2.92
Permeate (bar)	0.59	0.2	0.2	0.2	0.2	0.32	0.37	0.20	0.20
Ratio (P^{rt}/P^{pms})	3.17	4.48	2.78	7.85	3.56	3.68	3.29	5.17	3.12

Table 2 shows the resulting total membrane area and the power requirements of the three scenarios. The tradeoff between area and power in gas separation membrane networks is illustrated. The low membrane area observed for the optimisation run based on the co-current flow pattern is compensated by higher power consumption. The higher power consumption required results in the highest TAC, as shown in the table. An optimised co-current flow membrane-based CO_2 capture process would cost 18 % more than the optimised counter-current membrane-based CO_2 capture process. Optimisation based on the counter-current flow pattern results in 29.3 % savings in power consumption compared to the co-current flow pattern scenario. The counter-current flow pattern is more energy efficient due to an inbuilt transmembrane pressure difference along with the membrane profile. The CO_2 concentration is highest at the initial point of the membrane, whilst at the same point, the permeate is dilute due to the opposing directional flow of the components in the retentate and permeate sides. Uppaluri et al. (2004) also found that the counter-current configuration gave the lowest gas processing cost in their superstructure-based optimisation of the recovery of H_2 from syngas (H_2+CO_2). In the study, optimisation based on the cross-flow and counter-current pattern resulted in cost savings of 4.2 % compared to co-current flow in the membrane. In this work, the cross-flow pattern results in an 8.9 % cost reduction from the optimised co-current flow pattern membrane process. In this study, the cost of CO_2 capture increases by 18 % when optimisation is based on the co-current flow pattern compared to optimisation based on the counter-current flow, whilst only 6 % was realised in the work of Uppaluri et al. (2004). The higher cost difference realised can be attributed to the FSC membrane analysed in this work. The co-current flow pattern requires higher operating pressure; however, at high pressure, the CO_2 permeance decreases due to the carrier saturation phenomenon, further increasing the power requirements of the process.

Table 2: Optimum pressure and membrane area for the different membrane stages for the three scenarios

Parameter	Counter-current	Co-current	Cross-flow
Number of membrane stages	3	3	3
Recovery	0.9	0.9	0.9
Purity	0.95	0.95	0.95
Total membrane (x 10^6 m^2)	1.74	1.47	1.78
Total net power (MW)	171.14	221.4	190.8
Operating costs (US$)	51.4	66.5	57.4
Capital costs (x 10^6 US$)	89.4	100,3	95.8
TAC (x 10^6 US$/y)	140.8	166.8	153.2
CPU (s)	24	239	153

The optimised cross-flow pattern-based membrane process would cost 9 % more than the counter-current process design. Considering that the cost savings are not very significant, the cross-flow pattern would be recommended for large-scale applications since it is deemed the more practical.

4. Conclusions

The present study has explored the effect of the membrane flow pattern in the membrane module on superstructure-based optimisation of the FSC membrane process to the membrane flow pattern in gas separation process, specifically post-combustion CO_2 capture from power plants. The model developed considered the separation of multicomponent, humidified flue gas from a coal power plant. The process flow considered recycling of both permeate and retentate streams with the use of compressors on the membrane feed and vacuum on the permeate side. The objective of the optimisation was to minimise the total annualised cost of capture. The results show that the counter-current flow results in the most energy-efficient CO_2 capture process due to the innate partial pressure difference generated by the opposing flow directions of the retentate and the permeate. The energy savings difference is 29 % compared to the co-current flow pattern. The co-current flow pattern results in a smaller optimised membrane area which results in the cost being only 18 %

more than the counter-current. The co-current flow gives the least energy-efficient process and the highest cost of CO_2 capture process. This result is similar to the results observed for non-FSC membranes.

Nomenclature

A_{mem} – Membrane area of stage n m^2
$R^{fs}_{i,n}$ – flowrate of gas *i* in the membrane kmol/s
$R^{pms}_{i,n,k}$ – flowrate of *i* into k permeate kmol/s
$R^{pms}_{i,n}$ – flowrate of *i* on the permeate side kmol/s
$R^{rt}_{i,n}$ – flowrate of *i* from membrane on the retentate kmol/s
$R^{rt}_{i,n,k}$ – flowrate of *i* at point k of retentate kmol/s
$y^{rt}_{i,n,k}$ – flowrate of *i* on point k of retentate
$y^{pms}_{i,n,k}$ – mole fraction of *i* at k on the permeate

Acknowledgements

The authors would like to acknowledge the University of the Witwatersrand Research Office for support.

References

Arias A.M., Mussati M.C., Mores P.L., Scenna N.J., Caballero J.A., Mussati S.F., 2016. Optimization of multi-stage membrane systems for CO_2 capture from flue gas. Int. J. Greenh. Gas Control, 53, 371–390.

European Union, 2011. European best practice guidelines for assessment of CO_2 capture technologies, <https://www.ctc-n.org/sites/www.ctc-n.org/files/resources/d_4_9_best_practice_guide.pdf>, accessed 23/06/2022.

Chiwaye N., Majozi T., Daramola M.O., 2021. Optimisation of post-combustion carbon dioxide capture by use of a fixed site carrier membrane. Int. J. Greenh. Gas Control, 104, 103182.

Dai Z., Fabio S., Giuseppe Marino N., Riccardo C., Deng L., 2019. Field test of a pre-pilot scale hollow fiber facilitated transport membrane for CO_2 capture. Int. J. Greenh. Gas Control, 86, 191–200.

Hasan M.M.F., Baliban R.C., Elia J.A., Floudas C.A., 2012. Modeling, Simulation, and Optimization of Postcombustion CO_2 Capture for Variable Feed Concentration and Flow Rate. 1. Chemical Absorption and Membrane Processes. Ind. Eng. Chem. Res., 51, 1562–15664.

He X., Hägg M.-B., 2014. Energy Efficient Process for CO_2 Capture from Flue gas with Novel Fixed-site-carrier Membranes. Energy Procedia, 63, 174–185, DOI: 10.1016/j.egypro.2014.11.018.

Khalilpour R., Abbas A., Lai Z., Pinnau I., 2012. Modeling and parametric analysis of hollow fiber membrane system for carbon capture from multicomponent flue gas. AICHE J., 58, 1550–1561.

Kim T.-J., Vrålstad H., Sandru M., Hägg M.-B., 2013. Separation performance of PVAm composite membrane for CO_2 capture at various pH levels. J. Memb. Sci., 428, 218–224.

Lee S., Binns M., Kim J.-K., 2018. Automated process design and optimization of membrane-based CO_2 capture for a coal-based power plant. J. Memb. Sci., 563, 820–834.

Li S., Wang Z., He W., Zhang C., Wu H., Wang J., Wang S., 2014. Effects of Minor SO_2 on the Transport Properties of Fixed Carrier Membranes for CO_2 Capture. Ind. Eng. Chem. Res., 53, 7758–7767.

Liao J., Wang Z., Wang M., Gao C., Zhao S., Wang J., Wang S., 2016. Adjusting carrier microenvironment in CO_2 separation fixed carrier membrane. J. Memb. Sci., 511, 9–19.

Merkel T.C., Lin H., Wei X., Baker R., 2010. Power plant post-combustion carbon dioxide capture: An opportunity for membranes. J. Memb. Sci., 359, 126–139, DOI: 10.1016/j.memsci.2009.10.041.

Pfister M., Belaissaoui B., Favre E., 2017. Membrane gas separation processes from wet postcombustion flue gases for carbon capture and use: A critical reassessment. Ind. Eng. Chem. Res., 56, 591–602.

Puranik Y., Sahinidis N.V., 2017. Deletion presolve for accelerating infeasibility diagnosis in optimization models. INFORMS J. Comput., 29, 754–766.

Rautenbach R., Dahm W., 1987. Gas permeation — module design and arrangement. Chem. Eng. Process. Process Intensif., 21, 141–150.

Stoller M., Pulido J.M.O., 2017. Optimal design of membrane processes: A problem of choices between process layout, operating conditions and adopted control system. Chem. Eng. Trans., 57, 1087–1092.

Uppaluri R.V.S.S., Linke P., Kokossis A.C., 2004. Synthesis and Optimization of Gas Permeation Membrane Networks. Ind. Eng. Chem. Res., 43, 4305–4322.

Velasco J.A.C., Gooty R.T., Tawarmalani M., Agrawal R., 2021. Optimal Design of Membrane Cascades for Gaseous and Liquid Mixtures via MINLP. J. Memb. Sci., 636, 119514.

Yuan M., Liguori S., Lee K., Van Campen D.G., Toney M.F., Wilcox J., 2017. Vanadium As a Potential Membrane Material for Carbon Capture: Effects of Minor Flue Gas Species. Environ. Sci. Technol. 51, 11459–11467.

Zhang C., Wang Z., Cai Y., Yi C., Yang D., Yuan S., 2013. Investigation of gas permeation behavior in facilitated transport membranes: Relationship between gas permeance and partial pressure. Chem. Eng. J., 225, 744–751.